September 21, 2007

Infrared and X-Ray Evidence for Circumstellar Grain Destruction by the Blast Wave of Supernova 1987A

Eli Dwek[1], Richard G. Arendt [2], Patrice Bouchet[3], David N. Burrows[4], Peter Challis [5], I. John Danziger[6], James M. De Buizer[7], Robert D. Gehrz[8], Robert P. Kirshner[5], Richard McCray[9], Sangwook Park[4], Elisha Polomski[8], and Charles Woodward[8]

ABSTRACT

Multiwavelength observations of supernova remnant (SNR) 1987A show that its morphology and luminosity are rapidly changing at X-ray, optical, infrared, and radio wavelengths as the blast wave from the explosion expands into the circumstellar equatorial ring, produced by mass loss from the progenitor star. The observed infrared (IR) radiation arises from the interaction of dust grains that formed in mass outflow with the soft X-ray emitting plasma component of the shocked gas. *Spitzer* IRS spectra at 5 - 30 μm taken on day 6190 since the explosion show that the emission arises from $\sim 1.1 \times 10^{-6}\ M_{\odot}$ of silicate grains radiating at a temperature of $\sim 180\pm^{20}_{15}$ K. Subsequent observations on day 7137 show that the IR flux had increased by a factor of 2 while maintaining an almost identical spectral shape. The observed IR-to-X-ray flux ratio (IRX) is consistent

[1]Observational Cosmology Lab., Code 665; NASA Goddard Space Flight Center, Greenbelt, MD 20771, U.S.A., e-mail: eli.dwek@nasa.gov

[2]Science Systems & Applications, Inc. (SSAI), Code 665, NASA Goddard Space Flight Center, Greenbelt MD, 20771, U.S.A.

[3]DSM/DAPNIA/Service d'Astrophysique, CEA/Saclay, F-91191 Gif-sur-Yvette; Patrice.Bouchet@cea.fr

[4]Department of Astronomy and Astrophysics, Pennsylvania State University, 525 Davey Laboratory, University Park, PA 16802, U.S.A.

[5]Harvard-Smithsonian, CfA, 60 Garden St., MS-19, Cambridge, MA 02138, U.S.A.

[6]Osservatorio Astronomico di Trieste, Via Tiepolo, 11, Trieste, Italy

[7]Gemini Observatory, Southern Operations Center, c/o AURA, Casilla 603, La Serena, Chile

[8]Department of Astronomy, University of Minnesota, Minneapolis, MN 55455, U.S.A.

[9]Joint Inst. Lab. Astrophysics, University of Colorado, Boulder, CO 80309-0440, U.S.A.

with that of a dusty plasma with standard LMC dust abundances. This flux ratio has decreased by a factor of ~ 2 between days 6190 and 7137, providing the first direct observation of the ongoing destruction of dust in an expanding SN blast wave on dynamic time scales. Detailed models consistent with the observed dust temperature, the ionization fluence of the soft X-ray emission component, and the evolution of IRX suggest that the radiating silicate grains are immersed in a 3.5×10^6 K plasma with a density of $(0.3 - 1) \times 10^4$ cm^{-3}, and have a size distribution that is confined to a narrow range of radii between 0.02 and 0.2 μm. Smaller grains may have been evaporated by the initial UV flash from the supernova.

Subject headings: ISM: supernova remnants – ISM: individual (SNR 1987A) – ISM: interstellar dust – Infrared: general – X-rays: general

1. INTRODUCTION

On February 23, 1987, Supernova 1987A (SN 1987A), the brightest supernova since Kepler's SN in 1604, exploded in the Large Magellanic Cloud (LMC). About ten years thereafter, the energy output from the supernova became dominated by the interaction of its blast wave with the inner equatorial ring (ER), a dense ring of gas located at a distance of about 0.7 lyr from the center of the explosion, believed to be produced by mass loss from the progenitor star. The ER is being repeatedly observed at optical wavelengths with the *Hubble Space Telescope* (*HST*) (?), at X-ray energies with the *Chandra X-ray Observatory* (??), at radio frequencies with the Australian Telescope Compact Array (ATCA) (?), and in the mid-IR with the Gemini South observatory (??) and the *Spitzer* observatory (??). The morphological changes in its appearance in these different wavelength regimes (presented in Figure 6 of McCray 2007) reveal the progressive interaction of the SN blast wave with the ER. The interaction regions appear as hot spots in the *HST* images, representing the shocked regions of finger-like protrusions that were generated by Rayleigh-Taylor instabilities in the interaction of the wind from the progenitor star with the ER (see Figure 2 in McCray 2007).

The X-ray emission is thermal emission from the very hot plasma, and consists of two main characteristic components: a hard ($kT \approx 2$ keV) component representing a fast shock propagating into a low density medium, and a soft ($kT \approx 0.3$ keV) component representing a decelerated shock propagating into the denser protrusions (??). The optical emission arises from the gas that is shocked by the blast wave transmitted through the dense protrusions in the ER (?), and the radio emission is synchrotron radiation from electrons accelerated by the reverse shock (?). The mid-IR emission spectrum is comprised of line and continuum emission. The lines most probably originate from the optically bright dense knots. The continuum that dominates the spectrum is thermal emission from dust that was formed in the post main sequence wind of the progenitor star before it exploded. This dust could either be located in the shocked X-ray emitting plasma and heated by electronic collisions or in the optical knots and radiatively heated by the shocks giving rise to the optical emission (??). Dust has also formed in the ejecta of the supernova about 530 days after the explosion, as evidenced by optical and IR observations of SN1987A (????), but its current contribution to the total mid-IR emission is negligible (?).

Because the Gemini 11.7 μm image correlates well with both the X-ray and optical emission, the possibility that the dust is radiatively heated in the knots was considered in detail by ?. Estimated dust temperatures of $\sim$ 125 K fell short of the observed value of $\sim$ 180 K but given the uncertainties in the model parameters, this discrepancy could not firmly rule out this possible scenario for the location and heating mechanism of the dust. However, the combined IR and X-ray observations can be more readily explained if the dust resides in the shocked regions of the finger-like protrusions that give rise to the observed soft X-ray emission (?). We will adopt this scenario as our working hypothesis, and derive a self-consistent model for the composition, abundance, and size distribution of the dust to explain the evolutionary changes in the IR and X-ray fluxes resulting from the collisional heating and the destruction of the dust grains by the ambient plasma.

We first review the basic physical principles that determine the temperature of collisionally heated dust, and describe how the IR emission can be used to probe the physical condition of the X-ray emitting plasma. We also discuss what information can be derived from the comparison of the IR and X-ray fluxes from the gas (§2.1). The physics of dust particles in a hot gas is discussed in more detail by Dwek (1987) and Dwek & Arendt (1992). In §3 we present a simple analytical model for the evolution of the grain size distribution and total dust mass in the gas that is swept up by an expanding SN blast wave. In §4 we present *Spitzer* low resolution $5 - 30$ μm IRS spectra obtained on days 6190 and 7137 after the explosion. The IR spectra are used to derive the temperature and composition of the shock heated dust. We use IR and X-ray observations of the SN to constrain the grain size distribution and the time at which the SN blast wave first crashed into its dusty surroundings. The results of our paper are summarized in §5.

2. The Infrared Diagnostics of a Dusty X-ray Plasma

The morphological similarity between the X-ray and mid-IR images of SN 1987A suggests that the IR emission arises from dust that is collisionally heated by the X-ray emitting gas. Simple arguments presented below show that, under certain conditions, the IR luminosity and spectrum of a dusty plasma can be used as a diagnostic for the physical conditions of the gas and the details of the gas-grain interactions. Details of the arguments can be found in ? and ?.

2.1. The Dust Temperature as a Diagnostic of Electron Density

The collisional heating rate, $\mathcal{H}$(erg s^{-1}), of a dust grain of radius a embedded in a hot plasma is given by:

$$\mathcal{H} = \pi a^2 \sum_j n_j \; v_j \; \mathcal{E}_j \tag{1}$$

where n_j is the number density of the j-th plasma constituent, v_j, its thermal velocity, and $\mathcal{E}_j$ its thermally-averaged energy deposition in the dust. In all the following, we will assume that the ion and electron temperature are equal. Then $v_e \gg v_{ion}$, and the dust heating rate is dominated by electronic collisions.

Let E_{dep} be the thermally-averaged energy deposited by electrons in the solid. If most electrons are stopped in the dust then E_{dep} is, on average, equal to the thermal energy of the electrons, that is, $E_{dep} \propto T_e$, where T_e is the electron temperature. On the other hand, if most incident electrons go entirely through the grains, then E_{dep} is proportional to the electron stopping power in the solid, defined as $\rho^{-1}(dE/dx)$. At the energies of interest here the electronic stopping power has an energy dependence of $(dE/dx) \sim E^{-1/2}$ (?), or $dE \sim E^{-1/2}\, dx$ so that $E_{dep} \sim T_e^{-1/2}\, a$.

The functional dependence of the grain heating rate on gas density and temperature is then given by:

$$\begin{aligned} \mathcal{H} &\sim a^2 \; n_e \; T_e^{3/2} && \text{when electrons are stopped in the grain} \\ &\sim a^3 \; n_e && \text{when electrons gothrough the grain} \end{aligned} \tag{2}$$

where we used the fact that $v_e \sim T_e^{1/2}$.

The radiative cooling rate, $\mathcal{L}$, of the dust grain with temperature T_d by IR emission is given by:

$$\begin{aligned} \mathcal{L} &= \pi a^2 \; \sigma T_d^4 \; \langle Q \rangle \\ &\sim \pi a^3 \; \sigma T_d^{4+\beta} \end{aligned} \tag{3}$$

where σ is the Stefan-Boltzmann constant, and $\langle Q \rangle \propto a\, T_d^{\beta}$ is the Planck-averaged value of the dust emissivity, $Q(\lambda) \propto \lambda^{-\beta}$, where the value of emissivity index, β, is $\approx 1 - 2$.

In equilibrium, $\mathcal{H} = \mathcal{L}$, and the dust temperature dependence on plasma density and temperature can be written as:

$$\begin{aligned} T_d &\sim \left(\frac{n_e}{a}\right)^{\gamma} T_e^{3\gamma/2} && \text{when electrons are stopped in the grain} \\ &\sim n_e^{\gamma} && \text{when electrons gothrough the grain} \end{aligned} \tag{4}$$

where $\gamma \equiv 1/(4+\beta)$. These simple arguments show that when the gas temperature is sufficiently high, and the grain size sufficiently small so that most electrons go through the grain, the dust temperature depends only on the plasma density.

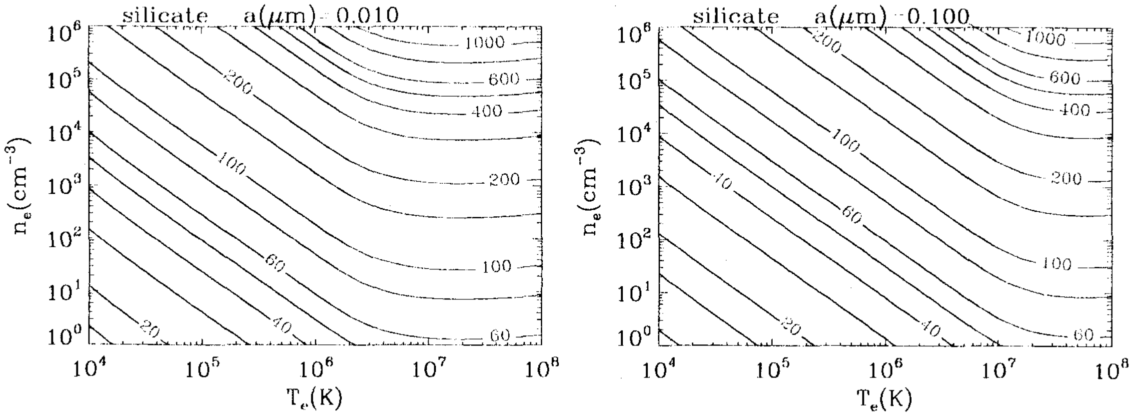

Fig. 1.— Contour plot of the equilibrium temperature of 0.01 μm (left) and 0.10 μm (right) silicate grains as a function of electron density and temperature. Above temperatures of $\sim 5\times10^6$ K the 0.01 μm grains become transparent to the incident electrons, and the dust temperature is only a function of electron density. The larger 0.1 μm grains become transparent only at electron temperatures above $\sim 3\times10^7$ K. We note here that a similar figure (Figure 15 in Bouchet et al. 2006) was mislabeled, and actually corresponds to contour levels of silicate dust temperature for grain radius of $a = 0.0030$ μm.

Figure ?? depicts contour levels of the dust temperature as a function of electron density and temperature for 0.01 μm and 0.10 μm silicate grains. The figure shows that above a certain gas temperature, its value depending on the grain radius, most of the electrons go through the grain and the dust temperature is essentially determined by the electron density. Under these conditions, the IR spectrum from the collisionally-heated grains becomes an excellent diagnostic of the density of the X-ray emitting gas.

2.2. The Stochastic Heating of Grains by Electronic Collisions

When dust grains are sufficiently small, a single electronic collision can deposit an amount of energy in the dust that is significantly larger that its enthalpy, causing a surge in

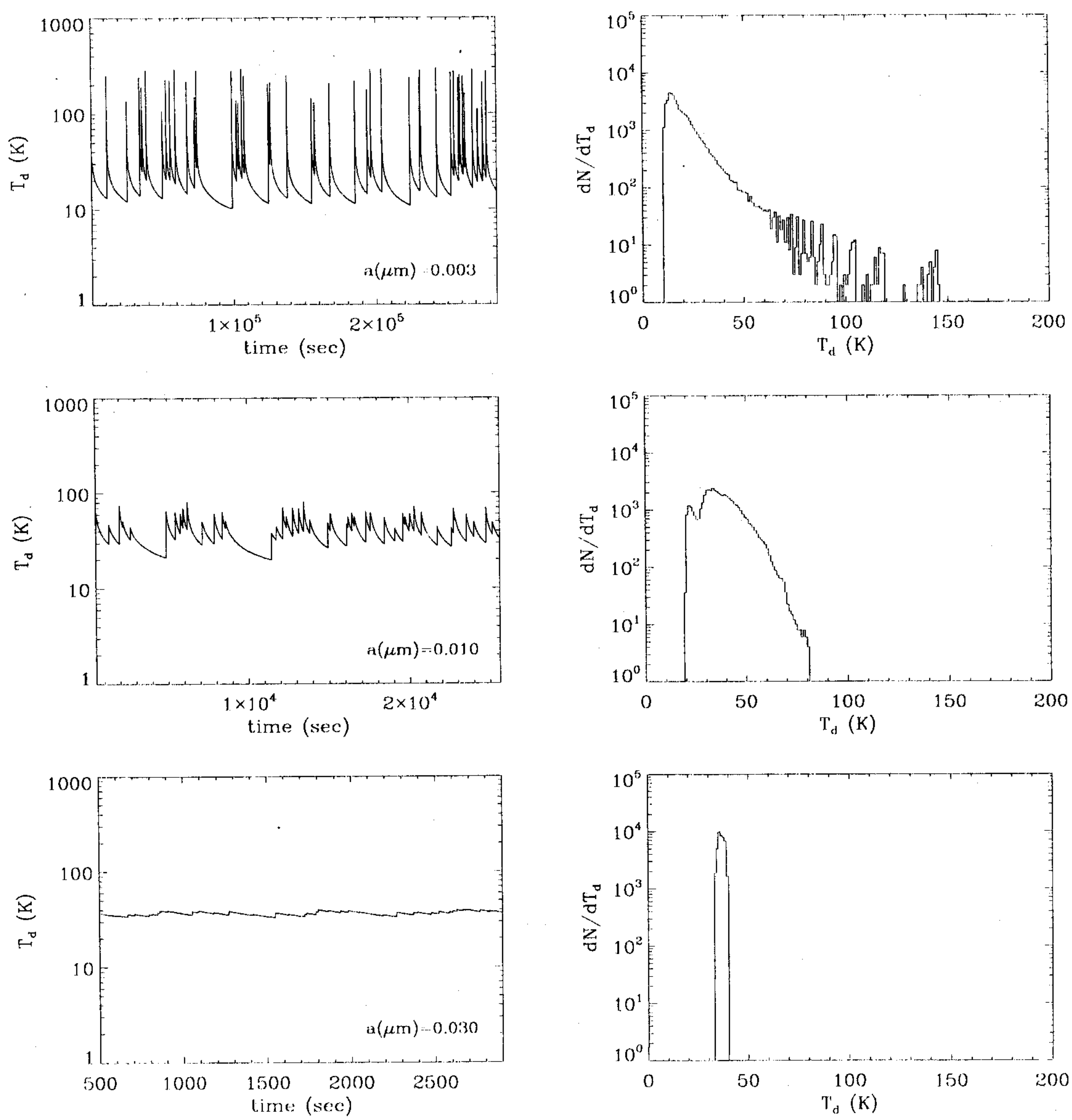

Fig. 2.— The stochastic heating of silicate grains in a hot X-ray emitting gas characterized by a temperature of $T_g = 10^6$ K, and electron density $n_e = 1$ cm^{-3} for dust grains of different radii. **Left column:** The temperature fluctuations as a function of time. **Right column:** The histogram of the fluctuations. As the grain size increases, the fluctuations get smaller, and the probability distribution of dust temperatures becomes strongly peaked around the equilibrium temperature of ~ 38 K.

dust temperature. If additionally, the time interval between successive electronic collisions is larger than the dust cooling time, the grain temperature will be fluctuating with time (??). Figure ?? depicts a simulation of the stochastic heating of 0.003, 0.01, and 0.03 μm silicate grains immersed in a hot X-ray emitting gas characterized a temperature $T_g = 10^6$ K, and an electron density $n_e = 1$ cm^{-3}. The left column shows the temperature fluctuations as a function of time, and the right column the histogram of the grain temperature. As the grain size increases, the fluctuations get smaller, and the histogram becomes strongly peaked around the equilibrium dust temperature of ~ 38 K, in this example.

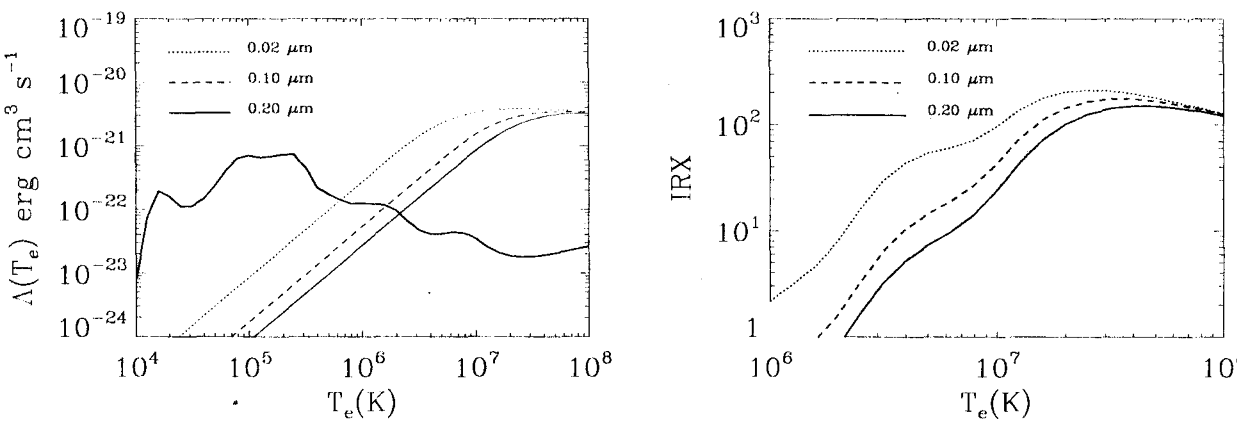

Fig. 3.— **Left panel**: The cooling function of a dusty plasma via atomic processes (thick solid line) and via gas grain collisions. Calculations were performed assuming a single-sized population of 0.02, 0.1 μm and 0.20 μm grains (solid line) with a dust-to-gas mass ratio of 0.0062, which is the value in the local ISM of the bare silicate-graphite+PAH dust model of ?. The gas cooling rate per unit volume for both processes is given by $L = n_e^2\, \Lambda(T)$. **Right panel**: The value of IRX for single-sized dust populations with radii of 0.02, 0.1, and 0.2 μm with the same dust-to-gas mass ratio as the figure on the left.

2.3. The Infrared to X-ray Flux Ratio

Another important diagnostic of a dusty plasma is IRX, defined as the ratio of the IR to X-ray fluxes emitted by the gas (Dwek et al. 1987). If the dust is collisionally-heated by the gas then the total IR flux, F_{IR}, emitted from a gas volume V is proportional to $n_e\, n_d\, \Lambda_d(T_g)\, V$, where n_d is the number density of dust particles, and $\Lambda_d(T_g)$ is the cooling function (units of erg cm^3 s^{-1}) of the gas via gas–grain collisions. The total X-ray flux, F_X, from the same volume is proportional to $n_e^2\, \Lambda_g(T_g)\, V$, where $\Lambda_g(T_g)$ is the cooling function of the gas via atomic processes. Thus

$$IRX \equiv \left(\frac{n_d}{n_e}\right) \frac{\Lambda_d(T_g)}{\Lambda_g(T_g)} \tag{5}$$

Both cooling functions represent the energy losses through collisional processes, characterized by $\langle \sigma\, v\, E \rangle$ summed over all interactions in the plasma, where σ is the cross section, v is the relative velocity of colliding species, and E is the energy lost in the process.

For a given dust-to-gas mass ratio, that is, a fixed (n_d/n_e) ratio, IRX depends only on plasma temperature. Figure **??** (left panel) shows the behavior of the atomic cooling function of a gas of solar composition as a function of gas temperature. Also shown in the figure is the gas cooling function via gas–grain collisions for a gas with a dust-to-gas atom mass ratio $Z_d = 0.0062$, and single-sized dust populations with radii of 0.02, 0.1, and 0.2 μm. The right panel of the figure presents the value of IRX for the same conditions. The figure shows that for soft X-rays ($kT_e \sim 0.3$ keV, $T_e \sim 3.5 \times 10^6$ K) this ratio varies between $\sim$ 3 and 20, depending on grain size. Each plasma temperature will have a different range of values, depending on the grain size distribution. Any deviation from these values will suggest that Z_d is either depleted or overabundant with respect to the reference value adopted in the calculations.

3. The Evolution of the Grain Size Distribution and Dust Mass

Consider the propagation of a shock into a dusty medium with a constant number density, n_0, and a fixed dust-to-gas mass ratio Z_d^0. The shocked gas can be regarded as a reservoir that is continuously being filled with gas and pristine dust by the expanding blast wave. If dust grains were not destroyed, the postshock gas would maintain a constant value Z_d^0 as the mass of shocked dust and gas evolve proportionally in time, with a functional dependence that depends on the geometry of the medium into which the blast wave is expanding. In the case where dust particles are destroyed by sputtering, the grain size distribution, and the dust-to-gas mass ratio in the shocked gas will evolve with time.

3.1. General Equations

A grain of radius a_0 that is swept up by the shock at some time t_0 will at time t be eroded to a radius $a(t)$ given by

$$a \equiv a(t) = a_0 + \int_{t_0}^{t} \left(\frac{da}{dt'}\right) dt' \tag{6}$$

where

$$\frac{da}{dt} \sim \sum_j n_j v_j Y_j < 0 \tag{7}$$

where Y_j is the thermally-averaged sputtering yield of the dust by the j-th gas constituent.

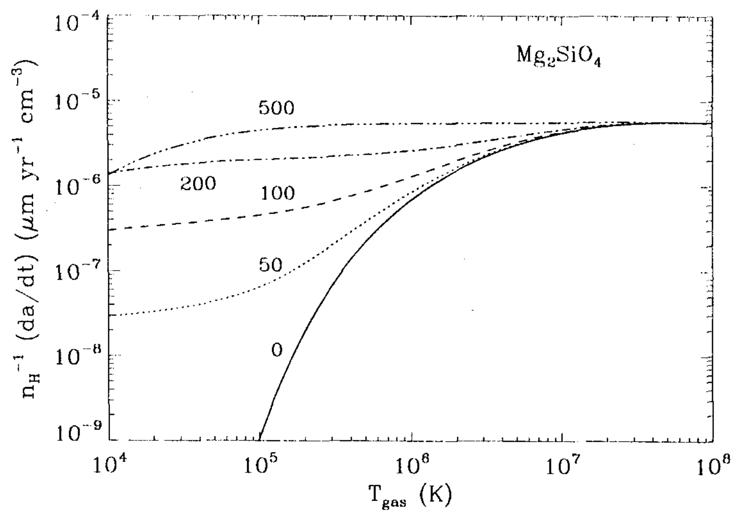

Fig. 4.— The absolute value of the sputtering rate of silicate (Mg_2SiO_4) dust grains moving through a hot gas of solar composition as a function of gas temperature. The curves are marked by the grain velocity (in km s^{-1}).

Dust particles swept up by a high velocity shock will move ballistically through the shock front and acquire a velocity relative to the shocked gas. The sputtering yield needs then to be averaged over a Maxwellian distribution of velocities that is displaced by the relative gas-grain motion from its origin in velocity space (?). Figure ?? shows the temperature dependence of the sputtering rate of silicate dust grains, calculated using sputtering yield parameters given by Nozawa et al. (2006), moving with velocity v_{gr} = 0, 50, 100, 200, and 500 km s^{-1} through a hot gas of solar composition. In contrast to the heating of grains, their erosion by thermal and kinetic sputtering is entirely done by the ionic constituents of the gas. For dust grains with velocities $\gtrsim$ 500 km s^{-1} and gas temperatures above $\sim 10^6$ K the sputtering rate is approximately constant and given by:

$$\begin{aligned} \frac{da}{dt} &\approx -5 \times 10^{-6}\, n_H(\mathrm{cm}^{-3}) \qquad \mu m\ \mathrm{yr}^{-1} \\ &\approx -1.4 \times 10^{-4}\, n_H(\mathrm{cm}^{-3}) \qquad \text{Å d}^{-1} \end{aligned} \tag{8}$$

If the shocked gas maintains a constant composition and density then a dust grain of initial radius a_0 that is swept up by the shock at some time t' will at time t have a radius a given by:

$$a = a_0 + \left(\frac{da}{dt}\right)(t - t') \tag{9}$$

Equation (??) can be written in dimensionless form as:

$$\xi = \xi_0 - \frac{(t - t')}{\tau_{max}} = \xi_0 - (\eta - \eta') \tag{10}$$

where $\xi \equiv a/a_{max}$, $\xi_0 \equiv a_0/a_{max}$, $\eta \equiv t/\tau_{max}$, $\eta' \equiv t'/\tau_{max}$, and

$$\tau_{max} \equiv a_{max} \, |da/dt|^{-1} \tag{11}$$

is the sputtering lifetime of the largest grain in the injected size distribution, which (using eq. ??) is numerically given by:

$$\begin{aligned} \tau_{max} &= 2 \times 10^5 \, \frac{a_{max}(\mu m)}{n_H(cm^{-3})} \quad \text{yr} \\ &= 7 \times 10^3 \, \frac{a_{max}(\mathring{A})}{n_H(cm^{-3})} \quad \text{d} \end{aligned} \tag{12}$$

Let n_d be the total number density of dust grains in the preshocked gas, and $n_d(a_0)\, da_0$, the number density of grains with radii between a_0 and $a_0 + da_0$. We assume that the grains have a size distribution in the pre-shocked gas given by:

$$n_d = \int_0^\infty n_d(a_0)\, da_0 \equiv n_d \int_0^\infty f(a_0)\, da_0 \tag{13}$$

where $f(a_0)$ is the normalized size distribution. If the grain size distribution extends over a limited range of radii, $a_{min} \leq a_0 \leq a_{max}$, then $f(a_0) = 0$ for any $a_0 < a_{min}$ or $a_0 > a_{max}$.

Dust grains are continuously injected into the shocked gas by the expanding SN blast wave. The total number of shocked grains with radii a in the $\{a,\, a + da\}$ interval at time t, $N_d(a,t)da$, is equal to the number of all dust particles of initial radius a_0 that were swept up at time t' $(0 \leqslant t' \leqslant t)$ and sputtered during the time interval $t' - t$ to radius a given by eq. (??). If $\dot{V}(t)$ is the growth rate of the volume of the shocked gas, then $N_d(a,t)$ can be written as:

$$N_d(a,\, t) = n_d \int_0^t \dot{V}(t')\, f(a_0)\, dt' \tag{14}$$

The lower limit of the integral, $t = 0$, corresponds to the time when the blast wave first encounters the dusty medium.

The total mass of shocked dust at any given time t is given by:

$$M_d(t) = \int_{a_{min}-|da/dt|t}^{a_{max}} m_d(a)\, N_d(a,t)\, da \tag{15}$$

where $m_d(a) = 4\pi\rho a^3/3$ is the mass of a dust grain of radius a.

Equation (??) can be written in dimensionless form:

$$N_d(\xi,\, \eta) = n_d \int_0^{\eta} \dot{V}(\eta')\, f(\xi + \eta - \eta')\, d\eta' \tag{16}$$

This integral is a convolution of the form: $\dot{V}(\eta') * f(\eta_0 - \eta')$, which can be numerically evaluated for arbitrary functions using Fourier transforms.

3.2. A Simple Analytical Solution

An analytical solution can be derived for a pre-shocked grain size distribution given by a power law in grain radius, and a power law time dependence of $\dot{V}$. We write the grain size distribution as:

$$\begin{aligned} f(a_0) &= C\, a_0^{-k} && a_{min} \le a_0 \le a_{max} \\ &= 0 && \text{otherwise} \end{aligned} \tag{17}$$

where $C \equiv (k-1)/(a_{min}^{-k+1} - a_{max}^{-k+1})$ is the normalization constant.
The time dependence of $\dot{V}(t')$ can be written as:

$$\dot{V}(t') = \dot{V}_0 \left(\frac{t'}{\tau_{max}}\right)^{\alpha} \tag{18}$$

where $\dot{V}_0$ is a proportionality constant, and $\alpha = 2$ for a spherical blast wave expanding into a uniform interstellar medium (ISM), and $\alpha = 0$ if the blast wave expands into a one-dimensional "finger-like" protrusion.

The total number density of grains in the $\{a, a + da\}$ radius interval is then given by:

$$N_d(a,t) = n_d\, \dot{V}_0 \int_0^{t} \left(\frac{t'}{\tau_{max}}\right)^{\alpha} f(a_0)\, dt' \tag{19}$$

Using eq. (??) to change variables from t' to a_0, eq. (??) can be rewritten as:

$$N_d(a,t) = \dot{N}_d \left|\frac{da}{dt}\right|^{-1} C \int_{a_{low}}^{a_{up}} \left[\left(\frac{t}{\tau_{max}} + \frac{a}{a_{max}}\right) - \left(\frac{a_0}{a_{max}}\right)\right]^{\alpha} a_0^{-k}\, da_0 \tag{20}$$

where $\dot{N}_d \equiv n_d \dot{V}_0$.

The time dependence of $N_d(a, t)$ is contained in the limits on the integral over the grain size distribution. If the radius a is within the range of the injected grain size distribution, that is, $a_{min} \leq a \leq a_{max}$, then $a_{low} = a$, since only grains with radii larger than a could have contributed to $N_d(a, t)$. If the radius a is smaller than a_{min}, then $N_d(a, t)$ is non-zero only if $a + |da/dt|t$ exceeds a_{min}, and $a_{low} = a_{min}$. In other words, the most recent injection of grains that could have contributed to $N_d(a, t)$ occurred at time $t - \Delta t$, where Δt is the time required to reduce the grain radius from a_{min} to a. The largest grains that could have been sputtered to radius a during the time t is equal to $a + |da/dt|t$. However, the largest grain size cannot exceed a_{max}, so the upper limit on the integral, a_{up}, is determined by the smaller of these two quantities. To summarize:

$$\begin{aligned} a_{low} &= \max\{a_{min},\ a\} \\ a_{up} &= \min\left\{a_{max},\ a + \left|\frac{da}{dt}\right| t\right\} \end{aligned} \tag{21}$$

For a shock expanding into a one-dimensional protrusion ($\alpha = 0$) the solution to eq. (??) is given by:

$$N_d(a, t)_{\alpha=0} = \dot{N}_d \left|\frac{da}{dt}\right|^{-1} \frac{\mathcal{C}}{(k-1)} \left[a_{low}^{-k+1} - a_{up}^{-k+1}\right] \tag{22}$$

At early times, when $t < a|da/dt|^{-1} \ll \tau_{max}$, $a_{up} = a$, and $a_{low} \approx a$, and the solution to eq. (??) becomes:

$$N_d(a, t)_{\alpha=0} = \dot{N}_d\, t\, \mathcal{C}\ a^{-k} \quad . \tag{23}$$

At late times, when $t > \tau_{max}$, $a_{up} = a_{max}$, and the asymptotic solution of (??) is:

$$\begin{aligned} N_d(a, t > \tau_{max})_{\alpha=0} &= \dot{N}_d \left|\frac{da}{dt}\right|^{-1} \frac{\mathcal{C}}{(k-1)} \left[a^{-k+1} - a_{max}^{-k+1}\right] \qquad a > a_{min} \\ &= \dot{N}_d \left|\frac{da}{dt}\right|^{-1} \frac{\mathcal{C}}{(k-1)} \left[a_{min}^{-k+1} - a_{max}^{-k+1}\right] = constant \qquad a \leq a_{min} \end{aligned} \tag{24}$$

For a shock wave expanding into a homogeneous medium (α=2) the solution is given by:

$$\begin{aligned} N_d(a, t)_{\alpha=2} = \ & \dot{N}_d \left|\frac{da}{dt}\right|^{-1} \mathcal{C} \left\{ \frac{1}{(k-1)} \left(\frac{t}{\tau_{max}} + \frac{a}{a_{max}}\right)^2 \left(a_{low}^{-k+1} - a_{up}^{-k+1}\right) \right. \\ & - \frac{2}{(k-2)} \left(\frac{t}{\tau_{max}} + \frac{a}{a_{max}}\right) \left(\frac{a_{low}^{-k+2} - a_{up}^{-k+2}}{a_{max}}\right) \\ & \left. + \frac{1}{(k-3)} \left(\frac{a_{low}^{-k+3} - a_{up}^{-k+3}}{a_{max}^2}\right) \right\} \end{aligned} \tag{25}$$

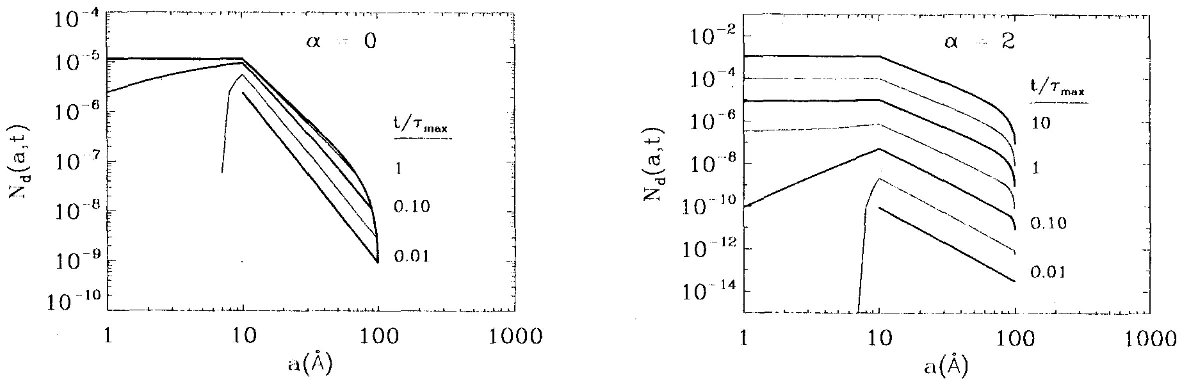

Fig. 5.— Evolution of the grain size distribution with time, measured in units of τ_{max}, the sputtering lifetime of the largest grain with radius a_{max} in the size distribution. Calculations were performed for a grain size distribution characterized by an $\sim a^{-3.5}$ power law in grain radii between 10 and 100 Å. The grain destruction rate, da/dt, was taken to be 0.14 Å d^{-1}. Bold lines are labeled by t/τ_{max}. **Left**: A spherical blast wave expanding into a one-dimensional protrusion ($\alpha = 0$). **Right**: A spherical blast wave expanding into a uniform ISM ($\alpha = 2$).

At late times, when $t \gg \tau_{max}$, the first term dominates, and the asymptotic solution of eq. (??) increases with time as t^2:

$$N_d(a, t > \tau_{max})_{\alpha=2} = \dot{N}_d \left|\frac{da}{dt}\right|^{-1} \frac{\mathcal{C}}{(k-1)} \left(\frac{t}{\tau_{max}}\right)^2 \mathcal{G}(a,t) \qquad (26)$$

where

$$\begin{aligned} \mathcal{G}(a,t) &\equiv \left[a^{-k+1} - a_{max}^{-k+1}\right] & & a > a_{min} \qquad (27) \\ &\equiv \left[a_{min}^{-k+1} - a_{max}^{-k+1}\right] = constant & & a \le a_{min} \end{aligned}$$

Figure ?? depicts the grain size distribution for different epochs. Select epochs, labeled by the dimensionless quantity t/τ_{max}, are represented by bold lines. Calculations were performed for an initial grain size distribution characterized by an $\sim a^{-3.5}$ power law in grain radius between 10 and 100 Å. The grain destruction rate, $|da/dt|$, was taken to be 0.14 Å d^{-1}, calculated for the sputtering rate of silicate grains in a hot gas with a temperature and density of $\sim 10^{6-8}$ K, and 1000 cm^{-3}, respectively

The figure illustrates the dependence of the evolution of the grain size distribution on the geometry of the ISM into which the blast wave is expanding. For a one-dimensional protrusion ($\alpha = 0$), the figure (left) shows a clear convergence of the size distribution to a fixed functional form and total number of grains for $t/\tau_{max} \gtrsim 1$. As the shock wave expands, the thickness of the shell of swept up dust increases with time. However, because of the finite grain lifetime, its thickness cannot exceed a value of $\Delta R_{sh} \approx v_{sh}\,\tau_{max}$, where v_{sh} is the shock velocity. So the grain size distribution and total mass reaches a steady state limit. When the blast wave expands into a uniform medium, the shell of shocked dust reaches the same steady state thickness ΔR_{sh}. However, since the surface of the shell increases as R_{sh}^2, where R_{sh} is the radius of the blast wave, the mass of shocked gas will continue to increase. This is clearly depicted in the right panel of the figure, which shows that $N_d(a, t)$ reaches a steady state, but continues to increase with time as t^2.

If grains were not sputtered in the shocked gas, then $N_d^0(a, t)\,da$, the total number of dust grains in the $\{a, a + da\}$ radius interval that are swept up by the shock at time t would be:

$$N_d^0(a,t)\,da = \dot{N}_d\,\tau_{max}\,\frac{\mathcal{C}}{(\alpha+1)}\left(\frac{t}{\tau_{max}}\right)^{\alpha+1} a^{-k}\,da \tag{28}$$

Their mass, M_d^0, is given by eq. (??) with $N_d(a, t)$ replaced by the expression above, and with $|da/dt|$ set to zero.

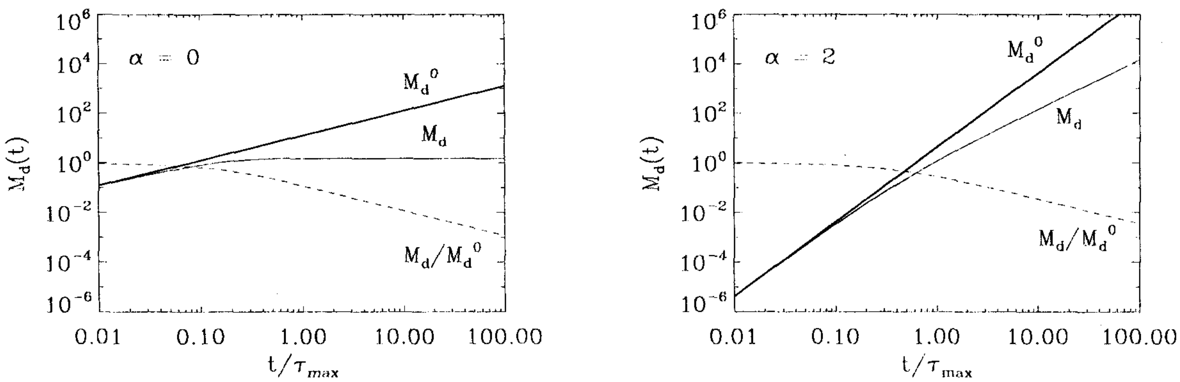

Fig. 6.— Evolution of the dust mass, M_d, the dust mass if grains were not sputtered, M_d^0, and the fraction of the surviving dust, M_d/M_d^0 with time, measured in units of τ_{max}, the sputtering lifetime of the largest grain in the size distribution $[\tau_{max}(d) = 7.3 \times 10^7\,a_{max}(\mu m)/n_H(cm^{-3})]$. Dust and gas parameters are identical to those used in Figure ??. The figure shows that the fractional change in M_d/M_d^0 between two epochs constrains the grain size distribution and the density of the X-ray emitting plasma. **Left**: A spherical blast wave expanding into a one-dimensional protrusion ($\alpha = 0$). **Right**: A spherical blast wave expanding into a uniform ISM ($\alpha = 2$).

Figure ?? shows the evolution of dust mass for a spherical blast wave expanding into a one-dimensional protrusion ($\alpha = 0$; left), and into a uniform ISM ($\alpha = 2$; right) as a function of t/τ_{max}. As explained above, when $\alpha = 0$, the mass of shocked dust, M_d, reaches a constant limit for $t \gg \tau_{max}$, whereas for $\alpha = 2$ the mass of the shocked dust will increase as t^2. If grains were not destroyed, the mass of swept up dust, M_d^0 would increase as t for $\alpha = 0$, and as t^3 for $\alpha = 2$. The figure also shows the evolution of the mass fraction of surviving dust grains, M_d/M_d^0. This mass fraction is proportional to the dust-to-gas mass ratio in the shocked gas, and for a constant gas temperature and density, it is also proportional to IRX, the IR-to-X-ray flux ratio in the shocked gas. The figure shows that the fractional change in M_d/M_d^0 between two epochs constrains the value of τ_{max} given in eq. (??) which in turn depends on the grain size distribution and the density of the X-ray emitting plasma. As a reminder, $\tau_{max}(d) = 7000\, a_{max}(\AA)/n_H(cm^{-3})$. For example, given a plasma density, the value of τ_{max} will depend only on a_{max}, the maximum grain radius. A small value of a_{max} will imply a low value for τ_{max}, so that large changes in M_d/M_d^0 occur over very short time scales. Conversely, large values of a_{max} and τ_{max}, will cause changes in M_d/M_d^0 to occur over very long time scales.

4. *Spitzer* Infrared Observations of SNR 1987A

4.1. The Evolution of the IR spectrum

Figure ?? shows the $5 - 30$ μm low resolution spectra of SNR 1987A taken on February 4, 2004 (day 6190 since the explosion), and on September 8, 2006 (day 7137 since the explosion) with the Infrared Spectrograph (IRS) (??) on board the *Spitzer* Space Telescope (??). Analysis of the spectrum taken on day 6190 revealed that the IR emission originated from $\sim 1.1 \times 10^{-6}\, M_\odot$ of silicate grains radiating at a temperature of $\sim 180^{+20}_{-15}$ K (Bouchet et al. 2006). These circumstellar grains were formed in the quiescent outflow of the progenitor star before it exploded. The total IR flux on day 6190 was 5.1×10^{-12} erg cm^{-2} s^{-1} (Bouchet et al. 2006), and increased after 947 days (day 7137)to 10.0×10^{-12} erg cm^{-2} s^{-1}. The right panel of figure ?? presents a comparison between the two spectra, both normalized to the same 10 μm intensity. The figure shows that the spectra are essentially identical, implying that the dust composition and temperature remained unchanged during the two observing periods. The lower curve in the figure is the ratio between the two spectra, emphasizing their similarity. The IR intensity increased by a factor of 2 between the two epochs.

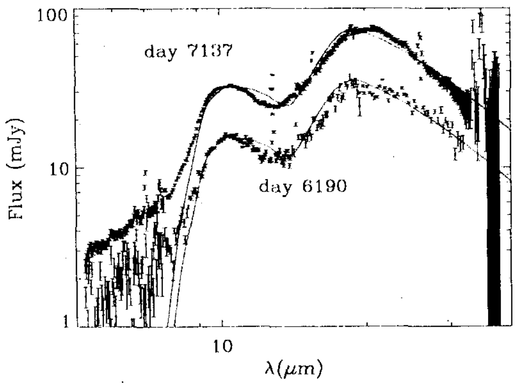

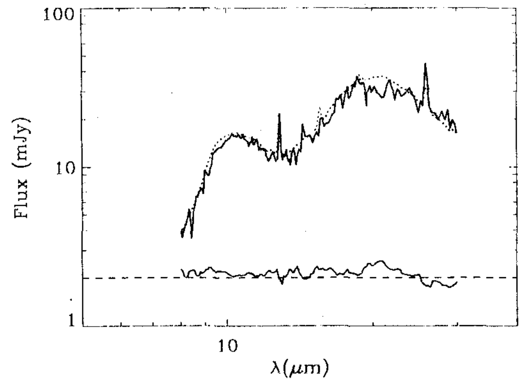

Fig. 7.— **Left**: The evolution of the IR spectrum of SN1987A from April 2, 2004 (day 6190 since the explosion) to September 8, 2006 (day 7137) taken with the *Spitzer* IRS (Bouchet et al. 2007; Arendt et al. 2007). **Right**: The smoothed spectra for days 6190 (solid line) and day 7137 (dashed line), normalized to the same brightness. The lower curve shows the ratio between the two spectra, with the horizontal line being the mean value. The figure shows that the dust spectrum increased by a factor of two between the two epoch, retaining essentially an identical spectrum corresponding to silicate grains radiating at an equilibrium temperature of 180^{+20}_{-15} K.

4.2. The IR-to-X-Ray Flux Ratio: Constraining the Dust Abundance in the ER

A comparison of the IR and X-ray fluxes provides strong constraints on the dust abundance in the shocked gas. X-ray fluxes taken between days 6157 and 7271 with the *Chandra* X-ray telescope (?) were interpolated for days 6190 and 7137 of the *Spitzer* observations. The total X-ray flux on day 6190, corrected for an extinction H-column density of $N_H = 2.35 \times 10^{21}$ cm^{-2}, is 2.1×10^{-12} erg cm^{-2} s^{-1}, half of it radiated by the slow shock component (?). The IR emission originates from the slow shock component which is penetrating the denser regions of the ER. This component comprises half of the observed X-ray flux. The resulting value of IRX on day 6190 is therefore 4.9 ± 1.1.

The theoretical value for IRX in a gas with LMC ISM abundances, taken here to be 0.6 times solar (?), ranges from about 2 to 12 for soft X-rays with $T_e \sim 3 \times 10^6$ K. The dust abundance in the ER is therefore consistent with LMC abundances. Since the silicon abundance in the ER should not have been altered by stellar nucleosynthesis, this agreement suggests efficient condensation of silicate grains in the presupernova outflow. The dust abundance on day 6190 is a lower limit on the original pre-SN value, since some of the dust may have been evaporated by the initial UV flash from the SN.

4.3. The IR-to-X-Ray Flux Ratio: The Effect of Prior Grain Destruction by the Initial UV Flash

HST images of the ER show that it is located at a distance of ~ 0.7 lyr (6.6×10^{17} cm) from the SN. At this distance small dust particles can be evaporated by the initial UV flash that emanated from the SN (?). Their calculations suggest that silicate dust particles with radius less than ~ 0.02 μm will be evaporated by the flash. A population of silicate grains with a $a^{-3.5}$ power law distribution in grain radius extending from 10 Å to 0.2 μm will loose about 30% of its mass. So had the flash not occurred, the value of IRX would have been ~ 7.

4.4. The Evolution of IR-to-X-Ray Flux Ratio: Evidence for Ongoing Grain Destruction by the SN Blast Wave

The IR flux increased by only a factor of ~ 2 from day 6190 to 7137. In comparison, the extinction-corrected 0.50-2.0 keV flux increased by a factor of ~ 3 during the same time period to a value of $\sim 6.4 \times 10^{-12}$ erg cm^{-2} s^{-1} (?). The fractional contribution of the soft X-ray component increased from 0.5 to 0.6, with no significant change in gas temperature ($kT \sim 0.3$ keV). All the increase in the soft X-ray flux can therefore be ascribed to an increase in the volume of the dense ($n_e \sim 10^4$ cm^{-3}) component of the ER that was shocked by the SN blast wave. The evolution in the X-ray and IR fluxes and the resulting value of IRX are summarized in Table 1. A similar evolutionary trend was reported by **??** although absolute values of IRX differ from those reported here because of differences in the X-ray energy bandpasses and dust models used in the calculations.

If grains were not destroyed, we would expect the IR intensity to increase by a similar factor. *The smaller increase in the IR flux, e.g. the decline in IRX, is a strong indicator that we are for the first time witnessing the actual destruction of dust in a shock on a dynamical timescale!* If the dust composition and size distribution is uniform throughout the region of the ER that has been swept up by the shock, then IRX is directly proportional to the dust-to-gas mass ratio, Z_d, or to M_d/M_d^0, the ratio between the actual mass of dust in the shocked gas, and the dust mass if grains were not destroyed. The magnitude of the decrease in IRX between the two epochs can therefore provide strong constraints on the grain size distribution in the preshocked gas of the ER, and the density of the X-ray emitting gas, which determines the rate of grain destruction.

4.5. Determining the Grain Size Distribution and Plasma Density

If the preshocked grain sizes are too large, then the fractional mass of the dust that could be destroyed during the time interval of 947 days will be too small to account for the observed decrease in the value of IRX. Conversely, if the grain sizes were too small, most of the dust mass would be destroyed, giving rise to a significantly larger than observed decrease in IRX between the two epochs. The right combination of grain sizes and gas densities is therefore required to produce the observed decrease in IRX and dust temperature. Furthermore, the small range of dust temperatures ($T_d \approx 165 - 200$ K) implied from the mid-IR spectrum of the ER also constrains the grains to a rather narrow range of sizes.

For a given gas temperature, the gas density is constrained by the size and temperature of the collisionally heated dust grains. The temperature of the soft X-ray component that heats the dust is about 3×10^6 K. If the dust grains are transparent to the incident electrons, then the dust temperature uniquely determines the gas density (see eq. ??). Inspection of Figure ?? suggests that 0.01 μm dust grains are transparent to electrons with mean temperatures above $\sim 3 \times 10^6$ K. The observed dust temperatures of 180 K then requires the electron density to be about $\sim 10^3$ cm^{-3}.

However, we do not know a priori if the dust grains are transparent to the incident electrons. If the grains are sufficiently large so that most of the incident electrons are stopped in the grains, then eq. (??) shows that for a given gas temperature, larger gas densities are required to obtain the same dust temperature that transparent grains would have. For example, Figure ?? (right) shows that gas densities of $\sim 10^4$ cm^{-3} are required to collisionally heat 0.1 μm dust grains to 180 K with a 3.5×10^6 K plasma.

The degeneracy between the different combinations of grain radii and plasma densities required to heat the dust to $\sim$ 180 K can be lifted by considering the additional observational constraints imposed by the evolution of IRX and the plasma ionization fluence derived from modeling the soft X-ray emission from the ER.

Figure ?? depicts the evolution in the $IRX(t_2)/IRX(t_1)$ ratio as a function of $t_1 - t_0$, where t_0 is the time, since the explosion, when the SN blast wave first crashed into the dense material of the ER, and where t_1 = 6190 d and t_2 = 7137 d correspond to the two epochs of near-simultaneous *Spitzer* and *Chandra* observations of the ER. The observed $IRX(t_2)/IRX(t_1)$ ratio is $\sim 0.53 \pm 0.16$ (see Table 1), and shown as a horizontal dashed line in the figure. The grain size distribution used in the calculations is characterized by a $a^{-3.5}$

power law in grain radii, extending from a minimum grain size of 10 Å to a value of a_{max} of 0.01, 0.04, and 0.1 μm. Results are presented for a SN blast wave expanding into a one dimensional protrusion ($\alpha = 0$, left column) and a uniform medium ($\alpha = 2$, right column) with densities of 10^3 cm^{-3} (top row) and 10^4 cm^{-3} (bottom row).

The figure shows that the $IRX(t_2)/IRX(t_1)$ ratio attains its lowest value when $t_1 - t_0$ is small, that is, when the first encounter of the ER with the SN blast wave occured just before t_1, the first epoch of *Spitzer* observations. Since t_1 is very close to t_0, very little grain destruction could have taken place during the $t_1 - t_0$ epoch. The value of $IRX(t_1)$ is therefore close to its pre-shock value. Consequently, any subsequent destruction would lead to relatively great changes in IRX at $t = t_2$. Conversely, $t_1 - t_0$ attains its largest value when $t_0 = 0$ (a physical impossibility because of the finite time required for the SN blast wave to reach the ER). Then, the relative change in IRX between the two epochs will be the smallest, and $IRX(t_2)/IRX(t_1) \rightarrow 1$.

Observationally, we can associate t_0 with the first encounter of the SN blast wave with the appearance of the first hot spot in the *HST* image from April 1997, about 3700 days after the explosion (?). The soft X-ray light curve shows that the rise could have occurred between days 3700 and 6000. The first epoch corresponds to the first appearance of the optical knots, and the latter epoch corresponds to the time when the flux from the soft X-ray component ($kT \sim 0.3$ keV) exceeded that from the hard component ($kT \sim 2$ keV) (?). From the mid-IR light curves (?), the energy output from the SN became ER dominated around day 4000. Adopting days 4000 to 6000 as a reasonable estimate for t_0 gives a range of possible values of $t_1 - t_0 \approx 200 - 2200$ d.

Inspection of Figure ?? illustrates the difficulty in constraining the grain size distribution or the astrophysical scenario (1-D protrusion or uniform ISM) because of the large uncertainty in the $IRX(t_2)/IRX(t_1)$ ratio, which ranges from 0.37 to 0.69, and the large range in $t_1 - t_0$. If we adopt the nominal value of $IRX(t_2)/IRX(t_1) = 0.53$, then the models clearly favor small grain sizes if $n_{gas} = 10^3$ cm^{-3}, regardless of the value of α, but are degenerate in the grain size distribution when $n_{gas} = 10^4$ cm^{-3}. The evolution the $IRX(t_2)/IRX(t_1)$ ratio alone is therefore not sufficient to lift the degeneracy in the different combinations of $\{n_e, a\}$ required to heat the dust to ~ 180 K.

However, the value of t_0 also determines the ionization age of the hot gas. The ionization fluence derived from modeling the soft X-ray spectra taken on days 6914, 7095, and 7271 is given by $n_e t_e \gtrsim 10^7$ cm^{-3} d (?). Taking t_0 to be between days 4000 and 6000 gives an ionization time $t_e \approx 1000 - 3000$ d, and corresponding electron densities $n_e \approx (10 - 3) \times 10^3$ cm^{-3}. These densities are high enough so that even small dust grains with radii ~ 10 Å will be collisionally heated to their equilibrium dust temperature. Furthermore, at these high densities, an equilibrium temperature of $\sim$ 180 K can only be reached if the soft X-ray electrons are stopped in the grains (see Figure ??). The narrow range of grain temperatures then suggests that the grain size distribution should have a narrow range as well, since $T_d \sim a^{-\gamma}$ (see eq. ??). The combined constraints on the gas density ($n_e \approx (0.3 - 1) \times 10^4$ cm^{-3}), gas temperature ($T_e \approx 3 \times 10^6$ K), and dust temperature ($T_d \approx 165 - 200$ K) can therefore be used to determine the range of grain sizes in the ER. From contour plots similar to Fig. 1, we find that the grain radii can be as small as 0.02 μm if the gas density is 3×10^3 cm^{-3}and as large as 0.2 μm if the gas density is 1×10^4 cm^{-3}. Dust temperatures for these two cases are 200 and 165 K, respectively.

A model consistent with the observed dust temperature, the ionization fluence of the soft X-ray emission component, and the evolution of the IRX ratio is depicted by the red curves in figure ??. They depict the evolution in the $IRX(t_2)/IRX(t_1)$ ratio for a population of silicate grains with a narrow $a^{-3.5}$ power law distribution in grain radius with $\{a_{min}, a_{max}\} = \{0.08, 0.1\}$ μm, in a gas with a density of 10^4 cm^{-3}. Taking the uncertainty in the $IRX(t_2)/IRX(t_1)$ ratio into account gives a value of $t_0 \approx 4200 - 5800$ d for $\alpha = 0$, consistent with X-ray and mid-IR observations. An lower limit of $t_0 \approx 4200$ d is inferred for the same dust model when the blast wave is propagating into a homogeneous medium.

4.6. Implications for Determining the Mass of the Circumstellar Environment of SN1987A Using Light Echoes

It is interesting to compare the dust properties derived for the ER with those derived for the progenitor's circumstellar environment from studies of the evolution and intensity of light echoes created by the scattering of the optical light from the supernova by the dust grains. At any given time, all points with equal delay time lie on an ellipsoid of revolution with the SN at one focal point and the observer at the other. Unfortunately, the ellipsoid at the earliest epoch at which the echoes were observed was outside the ER (see Figure 11n in ?). As a result, the light echoes probed only the circumstellar and interstellar media exterior to the ER.

Assuming cylindrical and reflection symmetry, ?? derived a model for the morphology of the scattering medium consisting of: (1) a peanut-shaped contact discontinuity (CD) between the red supergiant and main- sequence winds from the progenitor star; (2) a structure called Napoleon's Hat (NH) constituting the waist of this peanut; and (3) the two outer rings of the circumstellar shell (CS) that define the hourglass that is pinched by the ER. To model the scattered light ?? used the ? model for interstellar LMC dust with grain radii ranging from an upper limit of 0.2-2.0 μm to a lower limit of 0.00035 μm. By varying the relative silicate-to-carbon dust mass ratio while maintaining an LMC dust-to-gas mass ratio that is 0.3 times the value of the local interstellar medium, they estimated a total nebular mass of 1.7 $M_{\odot}$. They also found that the gas density increases, the maximum grain size decreases, and the silicate-to-carbon dust mass ratio increases as the echo samples material that is closer to the SN. The ER, with its population of smaller pure silicate grains, is consistent with this trend. The higher value of the minimum grain size in the ER may be the result of its proximity to the SN which caused the evaporation of grains smaller than 0.02 μm by the initial UV flash. Finally, the dust abundance in the ER is consistent with that adopted by ? for the nebula, supporting their derived value for the nebular mass.

5. Summary

The interaction of the SN 1987A blast wave with the complex structure of the ER has given rise to rapid evolutionary changes in the X-ray, optical and mid-IR morphology of the emission. The Gemini-S mid-IR images have established that the IR emission originates from dust in the ER that is swept up by the SN blast wave, and collisionaly heated by a soft X-ray component which has a temperature of $3.5\,10^6$ K, and an ionization fluence of $n_e t \gtrsim 10^7$ cm^{-3} d. The *Spitzer* infrared observations provide important complementary information on the evolution of the interaction of the SN blast wave with the ER and the properties of the dust in the hot X-ray emitting gas. The results of our analysis are as follows:

1. *Spitzer* spectral observations on day 6190 after the explosion revealed that the dust consists of silicate dust grains radiating at an equilibrium temperature of $\sim 180\pm^{20}_{15}$ K. Subsequent observations on day 7137 revealed that the IR flux increased by a factor of ~ 2, with the same dust composition and temperature remaining the same (Figure ??).

2. The dust grains could attain this temperature if they are sufficiently small ($a \sim 0.01$ μm) to be transparent to the incident electrons and are immersed in a relatively low density plasma with $n_e \sim 10^3$ cm^{-3}. Alternatively, the dust grains could be large enough to stop the incident electrons ($a \sim 0.1$ μm) if they are immersed in a higher density plasma with $n_e \sim 10^4$ cm^{-3}.

3. The degeneracy in the $\{n_e, a\}$ combinations required to heat the dust to ~ 180 K can be lifted by considering the additional constraints imposed by the observed evolution of the infrared-to-X-ray flux ratio (IRX) and by the ionization fluence obtained from modeling the soft X-ray emission component.

4. The value of IRX decreased by a factor of ~ 0.54 between days 6190 and 7137, suggesting that we are witnessing the effects of grain destruction on a dynamical timescale of the remnant. This decrease can be used to constrain the grain size distribution, time of impact of the SN blast wave with the ER, and the density of the X-ray emitting gas.

5. To follow the evolution of IRX, we constructed a model for the evolution of the grain size distribution in the shocked gas. In the model, pristine dust is continuously injected into the hot gas by the expanding SN blast wave, and destroyed by thermal and kinetic sputtering behind the shock. The evolution of the grain size distribution resulting from the combined effect of dust injection and destruction is presented in Figure ?? for different geometries of the medium into which the blast wave is expanding.

6. The evolution in IRX represents the changes in the dust-to-gas mass ratio in the shocked gas resulting from grain destruction (see Figures ?? and ??). A given decrease in IRX between two epochs constrains the epoch at which the dust is first swept up by the SN blast wave (which determines the ionization time), the plasma density, and the grain size distribution. Given a plasma density, if the grains are too small they will be rapidly destroyed, giving rise to large changes in IRX on short time scales. Conversely, if the grains are too large, the interval of time over which IRX drops by the observed factor will become too long.

7. A self-consistent picture that emerges from the application of the model to the combined X-ray and IR observations is that of a SN blast wave expanding into a dusty finger-like protrusion of the ER. The dust in the preshocked gas consists of pure silicate dust with a normal LMC dust-to-gas mass ratio and a grain size distribution limited to radii between 0.02 and 0.2 μm, sufficiently large to stop the incident electrons. Smaller grain sizes may have formed in the mass outflow from the progenitor star but were probably vaporized by the initial UV flash from the SN. The SN blast wave crashed into the ER between days 3600 and 6000 after the explosion giving rise to the observed soft X-ray emission. Typical temperatures and densities of the soft X-ray emitting gas are $\sim 3 \times 10^6$ K and $(0.3 - 1) \times 10^4$ cm^{-3}, consistent with those required to collisionally heat the dust to a temperature of $\sim$ 180 K. The plasma parameters and grain size distribution are consistent with the amount of grain destruction needed to account for the observed decrease in the IRX flux ratio between days 6190 and 7137. At these gas densities, the onset of grain destruction occurred about 1200 – 2000 days before the first *Spitzer* observations, consistent with the rise in the soft X-ray flux and the ionization time derived from X-ray models. The absolute value of IRX is consistent with that expected from a dusty plasma with a typical LMC dust-to-gas mass ratio, taken here to be 60% of the value of the local ISM.

Further Gemini and *Spitzer* observations of SNR 1987A are in progress which, with combined X-ray observations, will shed further light on the nature of the morphology and dust properties of the circumstellar medium around the SN.

This work is based on observations made with the *Spitzer* Space Telescope, which is operated by the Jet Propulsion Laboratory, California Institute of Technology, under a contract with NASA. E.D. acknowledges partial support from HST grant GO-9114 for the Supernova INtensive Survey (SINS: Robert Kirshner, PI), and by NASA OSS LTSA-2003-0065. The work of R.G.A. was supported by a grant awarded to Spitzer Cycle 3 proposal ID 30067. R.D.G. was supported by NASA through contract No. 1215746 issued by JPL/Caltech to the University of Minnesota. S.P. was supported in part by the SAO under Chandra grants GO5-6073X and GO6-7047X.

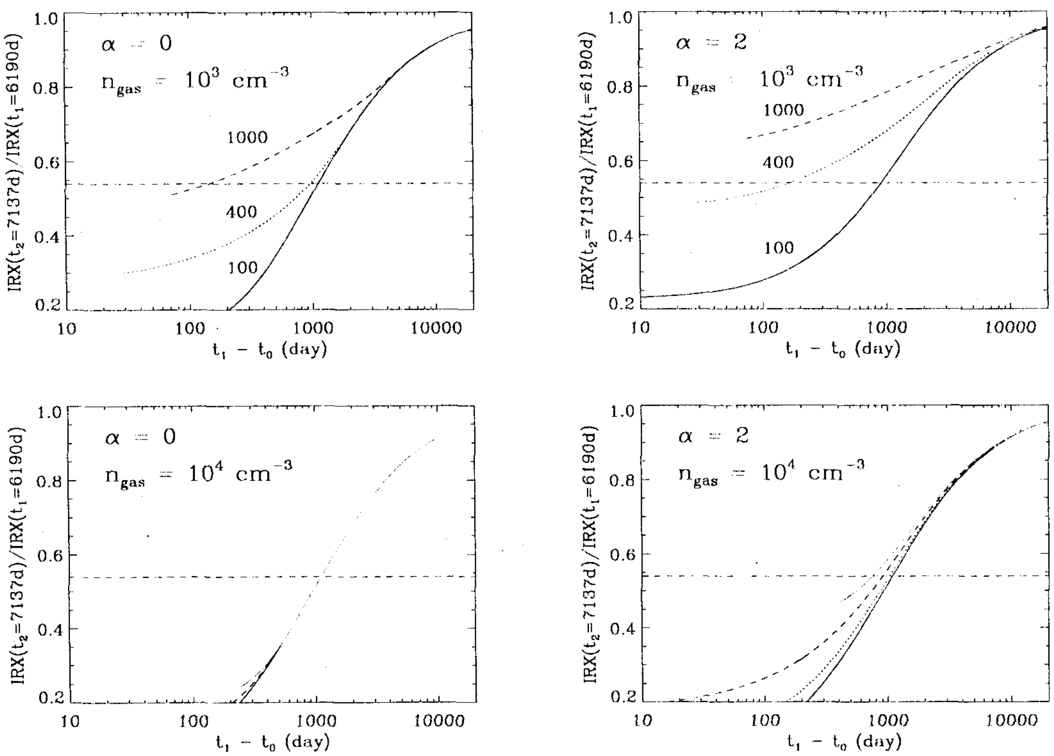

Fig. 8.— Evolution of the ratio $IRX(t_2)/IRX(t_1)$ as a function of the time difference $t_1 - t_0$. The time t_0 is the time since the explosion when the SN blast wave first encountered the dusty equatorial ring (ER). The times t_1 and t_2 correspond to the two epochs of near-simultaneous *Spitzer* and *Chandra* observations of the ER, respectively, days 6190 and 7137 since the explosion. The dashed horizontal line depicts the nominal value of the $IRX(t_2)/IRX(t_1)$ ratio which is 0.53 ± 0.16 (see Table 1). The curves are labeled by the maximum grain size (in Å) of the distribution. The minimum grain size was taken to be 10 Å in all cases. The red curves correspond to a narrow grain size distribution with $\{a_{min}, a_{max}\} = \{800, 1000\}$ Å. Figures are also labeled by the value of n_{gas}, the density of the shocked gas. **Left column**: A spherical blast wave expanding into a one-dimensional protrusion ($\alpha = 0$). **Right column**: A spherical blast wave expanding into a uniform ISM ($\alpha = 2$).

Table 1. Observed X-ray and Infrared Fluxes From SN 1987A

day number[1]	X-ray flux[2]	f_{soft}[3]	IR flux	IRX flux ratio[4]
6190	$(2.1 \pm 0.32)\,10^{-12}$	0.50	$(5.1 \pm 0.9)\,10^{-12}$	4.9 ± 1.1
7137	$(6.4 \pm 0.32)\,10^{-12}$	0.60	$(1.0 \pm 0.18)\,10^{-11}$	2.6 ± 0.5

[1]Since the explosion

[2]X-ray flux in the 0.5-2.0 keV band, interpolated to the epochs of the *Spitzer* observations and corrected for an extinction column density of $N_H = 2.35\,10^{21}$. The error represents the uncertainty in the pile up correction factor (Park et al. 2007).

[3]The fraction of the 0.5-2.0 keV flux that arises from the soft ($kT \sim 0.3$ keV) X-ray component (?).

[4]The ratio of the IR to soft X-ray flux from the SN. The IRX flux ratio has decreased by a factor of 0.53 ± 0.16 from day 6190 to day 7137.